ADVANCED MATERIALS TECHNOLOGIES
www.advmattechnol.de

Efficient Continuous Light-Driven Electrochemical Water Splitting Enabled by Monolithic Perovskite-Silicon Tandem Photovoltaics

*Kunal Datta, Bruno Branco, Yifeng Zhao, Valerio Zardetto, Nga Phung, Andrea Bracesco, Luana Mazzarella, Martijn M. Wienk, Mariadriana Creatore, Olindo Isabella, and René A. J. Janssen**

Solar-assisted water electrolysis is a promising technology for storing the energy of incident solar irradiation into hydrogen as a fuel. Here, an integrated continuous flow electrochemical reactor coupled to a monolithic perovskite-silicon tandem solar cell is demonstrated that provides light-driven electrochemical solar-to-hydrogen conversion with an energy conversion efficiency exceeding 21% at 1-Sun equivalent light intensity and stable operation during three simulated day-night cycles.

1. Introduction

Energy storage is a core element in a decarbonized energy economy as it helps overcome the intermittency of wind and solar energy, thereby ensuring a reliable supply of renewable power, where solar electricity plays a key role.[1] Electrochemical water splitting is one such technique that allows the direct conversion of electrical power to high energy density hydrogen (H_2) fuel. However, present-day H_2 production relies on the byproducts of fossil fuel extraction to generate industrial H_2 which invariably has a high associated carbon cost.[2,3] Alternatively, by using photovoltaic (PV)-assisted electrochemical water splitting to convert incident solar energy to H_2, H_2 production can be accomplished with a lower carbon footprint. Achieving a high solar-to-hydrogen efficiency (STH) using low-cost light-absorbing components remains a key determinant to the cost of H_2 generation,[4] thereby determining the commercial competitiveness of electrochemical systems to conventional methods.

Figure 1 shows recent trends in the laboratory-scale development of solar-assisted water splitting technology using integrated electrochemical and photovoltaic systems (references in Table S1, Supporting Information). Batch systems using standard H-cells can be built in combination with photovoltaic devices operated at lower light intensities due to the lower current output. For instance, STH efficiency >21% (at 0.35-Sun equivalent light intensity) has been reported for an integrated system using an InGaP/GaAs/Ge triple-junction solar cell and ruthenium-based molecular water-oxidation catalysts.[5] Continuous flow electrochemical cells (ECs), however, can achieve higher operating currents due to the use of thin solid-state electrolytes that have higher ionic conductivity in comparison to liquid electrolytes commonly used in H-cells and reduced inter-electrode distance (<100 μm), reducing ohmic losses.[6] Furthermore, the constant water flow avoids the accumulation of gaseous products at the electrode's surface, allowing higher currents to be achieved at lower potentials.[7] Hence, common water splitting systems using inorganic multijunction PV cells and continuous flow ECs typically use light concentration techniques in order to reach the high current output. For instance, STH efficiency of 30% has been reported using a InGaP/GaAs/GaInNAsSb triple-junction solar cell operated at 42-Sun equivalent light intensity, coupled to a Ir/Pt catalyst combination for the anode/cathode sub-cells in the flow EC series.[8]

Lead halide perovskite-based multijunction solar cells promise a cost-effective route to increase power conversion efficiency (PCE) due to the comparatively inexpensive material

K. Datta, B. Branco, M. M. Wienk, R. A. J. Janssen
Molecular Materials and Nanosystems
Institute of Complex Molecular Systems
Eindhoven University of Technology
P.O. Box 513 MB, Eindhoven 5600, The Netherlands
E-mail: r.a.j.janssen@tue.nl

Y. Zhao, L. Mazzarella, O. Isabella
Photovoltaic Materials and Devices group
Delft University of Technology
CD, Delft 2628, The Netherlands

V. Zardetto
TNO-partner in Solliance
High Tech Campus 21, AE, Eindhoven 5656, The Netherlands

N. Phung, A. Bracesco, M. Creatore
Department of Applied Physics
Eindhoven University of Technology
P.O. Box 513 MB, Eindhoven 5600, The Netherlands

M. Creatore
Eindhoven Institute of Renewable Energy Systems (EIRES)
P.O. Box 513 MB, Eindhoven 5600, The Netherlands

R. A. J. Janssen
Dutch Institute for Fundamental Energy Research
De Zaale 20, AJ, Eindhoven 5612, The Netherlands

The ORCID identification number(s) for the author(s) of this article can be found under https://doi.org/10.1002/admt.202201131.

DOI: 10.1002/admt.202201131

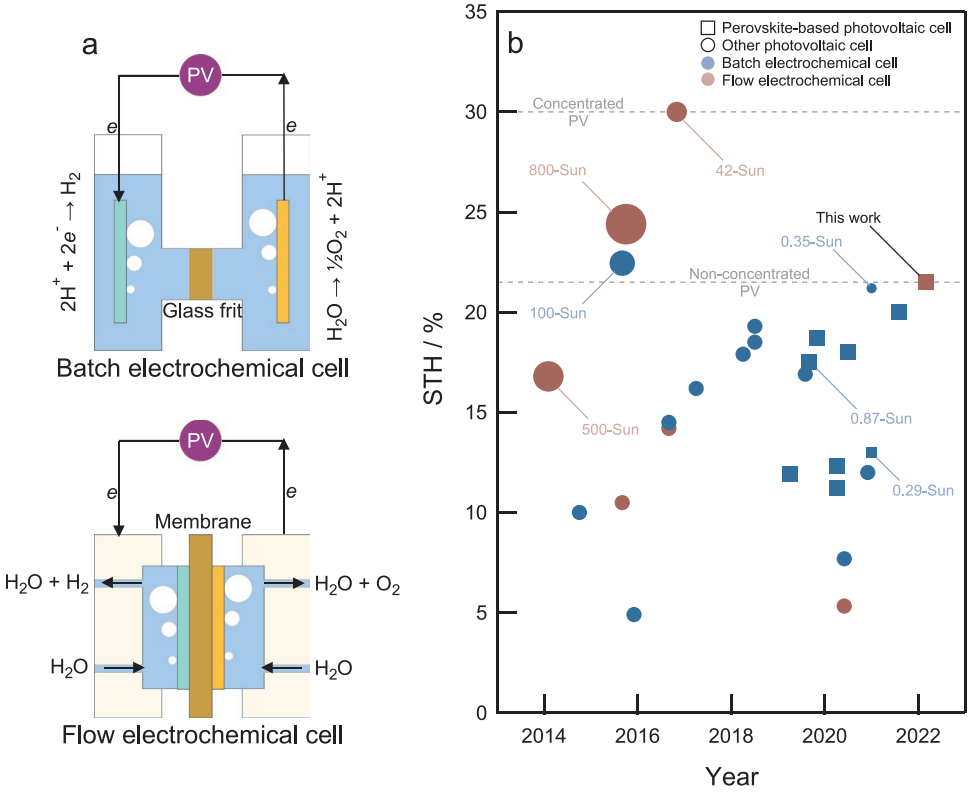

Figure 1. Development of photovoltaic-based water splitting systems. a) Schematics of (top) static H-cell and (bottom) continuous flow electrochemical cell-based devices. b) Solar-to-hydrogen efficiency across different classes of electrochemical cells driven by perovskite-based or other photovoltaic devices. The color of the marker distinguishes batch (blue) or flow (red) electrochemical cells, the shape indicates perovskite-based (square) or other photovoltaic devices (circle), and the size emphasizes illumination intensity. Unless specified, all the devices are operated at approx. 1-Sun equivalent light intensity.

and processing costs associated with perovskite-based solar cells. Furthermore, the high luminescence quantum efficiency of such materials allows for achieving high open-circuit voltage (V_{oc}) in devices. As a result, by combining wide-bandgap perovskite semiconductors with narrow-bandgap crystalline silicon (c-Si) bottom cells, multijunction devices are projected to exceed 30% PCE in the near future.[9,10] As one-half of PV-assisted water splitting systems, such devices are especially interesting because their high V_{oc} enables a high current output at the required operating potential (>1.23 V). In static EC systems based on H-cells, perovskite-based multijunction cells have been used to deliver high STH efficiency, reaching over 18% based on monolithic perovskite-silicon, 20% with stacked perovskite-silicon, and over 12% using monolithic perovskite-organic tandem devices.[11–13]

In this work, we report a light-driven continuous flow water splitting device, powered by a 1 cm^2 monolithic perovskite-silicon tandem solar cell operated at 1-Sun equivalent light intensity. The good compatibility between the electrical behavior of the PV and EC components results in a STH efficiency >21%, exceeding previously reported values at 1-Sun, together with stable operation during 72 h of diurnal operation.

2. Results and Discussion

An electrochemical flow cell with an active area of 4 cm^2 was constructed based on a two-compartment design; the compartments are separated by a Nafion NRE-212 membrane (50 µm thickness) coated with 1.2 mg cm^{-2} Pt and 2.0 mg cm^{-2} RuO_2 for hydrogen and oxygen evolution respectively (**Figure 2**a). The membrane-electrode assembly (MEA), along with titanium (anode) and carbon (cathode) porous transport layers (PTLs), is pressed between two titanium plates with parallel flow fields that act as current collectors and fluid distributors. Figure 2b shows the cross-section scanning electron microscopy (SEM) image of the MEA. The thickness of Pt/C layer is about 30 ± 2 µm and the RuO_2 layer has a thickness of 16 ± 2 µm; the total thickness of the MEA is ≈100 µm. The reduced inter-electrode distance grants decreased ohmic loss, and accordingly, higher currents can be more easily achieved.

The polarization curve of the EC at room temperature (Figure 2c) shows that a cell voltage of 1.42 V is measured at an applied current of 20 mA (J_{EC} = 5 mA cm^{-2}). However, the potential only slightly increases to 1.60 V when the applied current is increased to 1500 mA (J_{EC} = 375 mA cm^{-2}). The small increase in potential at a high current density range allows the solar-assisted water splitting system to operate within a narrow potential window, independent of solar illumination intensity, minimizing the degradation of the catalysts and electrodes.[14,15] Furthermore, the EC cell is operationally stable when applying a constant current of 18.0 mA (J_{EC} = 4.5 mA cm^{-2}) as shown in Figure 2d. Finally, hydrogen evolution, as quantified by in-line gas chromatography, was found to be similar to that determined theoretically (Figure S1, Supporting Information). As a

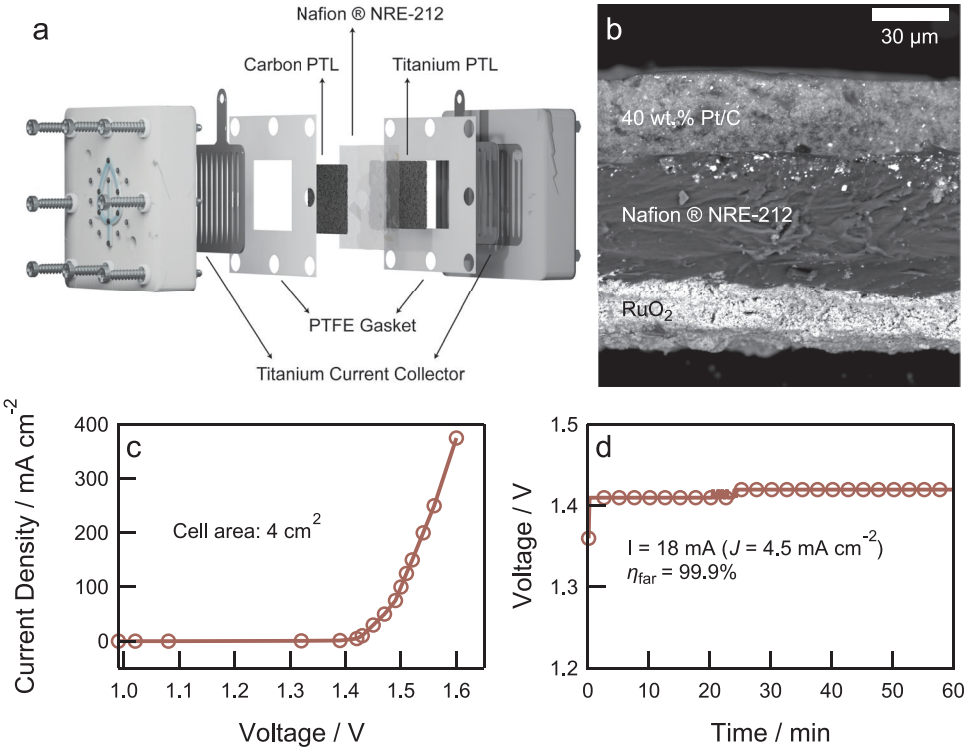

Figure 2. Electrochemical flow cell. a) Schematic of the electrochemical flow cell assembly indicating the membrane, PTLs, Teflon (PTFE) gaskets, and titanium current collectors. b) Cross-section SEM image of a representative MEA. The hydrogen (Pt) and oxygen (RuO_2) evolution sides are identified. c) Polarization curve of the electrochemical flow cell (active area = 4 cm^2, Pt/Nafion NRE-212/RuO_2) using ultrapure water at room temperature. d) Galvanostatic measurement at I = 18.0 mA for 1 h.

result, under operating conditions, the flow EC has a Faradaic efficiency (η_{far}) close to unity (0.999).

Monolithic perovskite-silicon tandem solar cells (**Figure 3**a) were prepared using a wide-bandgap ($E_g \approx 1.67$ eV) perovskite (nominally $K_{0.05}Cs_{0.05}(FA_{0.79}MA_{0.21})_{0.90}Pb(I_{0.79}Br_{0.21})_3$) top-cell integrated with a silicon heterojunction (SHJ) bottom-cell. The perovskite top-cell was fabricated using an atomic layer deposited (ALD) NiO interlayer and a self-assembled monolayer (SAM) of [2-(9H-carbazol-9-yl)ethyl]phosphonic acid (2PACz) as hole-selective contact, and a thermally evaporated C_{60} layer as electron-selective contact. The perovskite/C_{60} interface was treated with choline chloride to reduce interfacial defects and improve the V_{oc} of the perovskite sub-cell.[16,17] The SHJ device platform was chosen for the bottom-cell because of the high achievable V_{oc} (0.70 V) which makes it commonly used in efficient perovskite-silicon tandem structures.[18] Photovoltaic performances of representative *p-i-n* perovskite and SHJ single-junction solar cells are shown in Figure S2 and Table S2 (Supporting Information). The perovskite top-cell and c-Si bottom-cell were monolithically integrated using an indium tin oxide (ITO) interconnection layer. Figure 3b shows the X-ray photoelectron spectra (XPS) in the oxygen (O1s) region of the ITO surface which allows quantifying the ratio between hydroxyl (–OH) and metal oxide (M–O) species at the ITO surface. As can be seen, transparent ITO electrodes on glass (commercial ITO) used to prepare single-junction solar cells have an –OH to M–O ratio of 0.61 (Figure 3c). In contrast, the –OH to M–O ratio of the ITO layer deposited in-house (sputtered ITO) has a lower –OH to M–O ratio of 0.57.

Tandem cells made using a 2PACz SAM directly on the sputtered ITO interlayer showed a V_{oc}^{tandem} of 0.74 V (Figure 3d), i.e., close to V_{oc}^{c-Si} of an SHJ single-junction device. The low V_{oc}^{tandem} indicates a partial coverage of the 2PACz SAM, which binds to metal oxide surfaces through a phosphonic acid anchoring group,[19] leading to a poorly-functioning hole-selective contact in the perovskite top-cell. This was solved by depositing a thin (≈8 nm) NiO layer on the sputtered ITO using ALD.[20] Subsequent XPS characterization showed that the –OH to M–O ratio increased from 0.57 for the ITO surface to 0.70 for the NiO surface. The increased hydroxyl surface concentration, and thereby improved 2PACz coverage, resulted in a significantly higher V_{oc}^{tandem} of 1.78 V, approaching the sum of V_{oc}^{c-Si} and $V_{oc}^{perovskite}$. A champion device with a stable PCE of 25.1% (J_{sc} = 17.9 mA cm^{-2}, V_{oc} = 1.80 V, FF = 0.78) with minimal mismatch in short-circuit current density (J_{sc}) between the two sub-cells (Figure 3e,f) can therefore be prepared, aided by the ALD-NiO layer.

The electrochemical and photovoltaic cells were wire-connected into an integrated solar-assisted water-splitting system. Here, the overlap between the polarization curve (EC) and current density versus voltage curve (PV) determines the operating point of the system (1.41 V and 17.5 mA) at 1-Sun equivalent light intensity (**Figure 4**a).[12,13,21,22] Under these conditions, the system is operating below the thermoneutral potential for water splitting (E_{tn}^0 = 1.48 V); thus, the remaining energy (0.07 V) is provided by the water flowing in the electrochemical

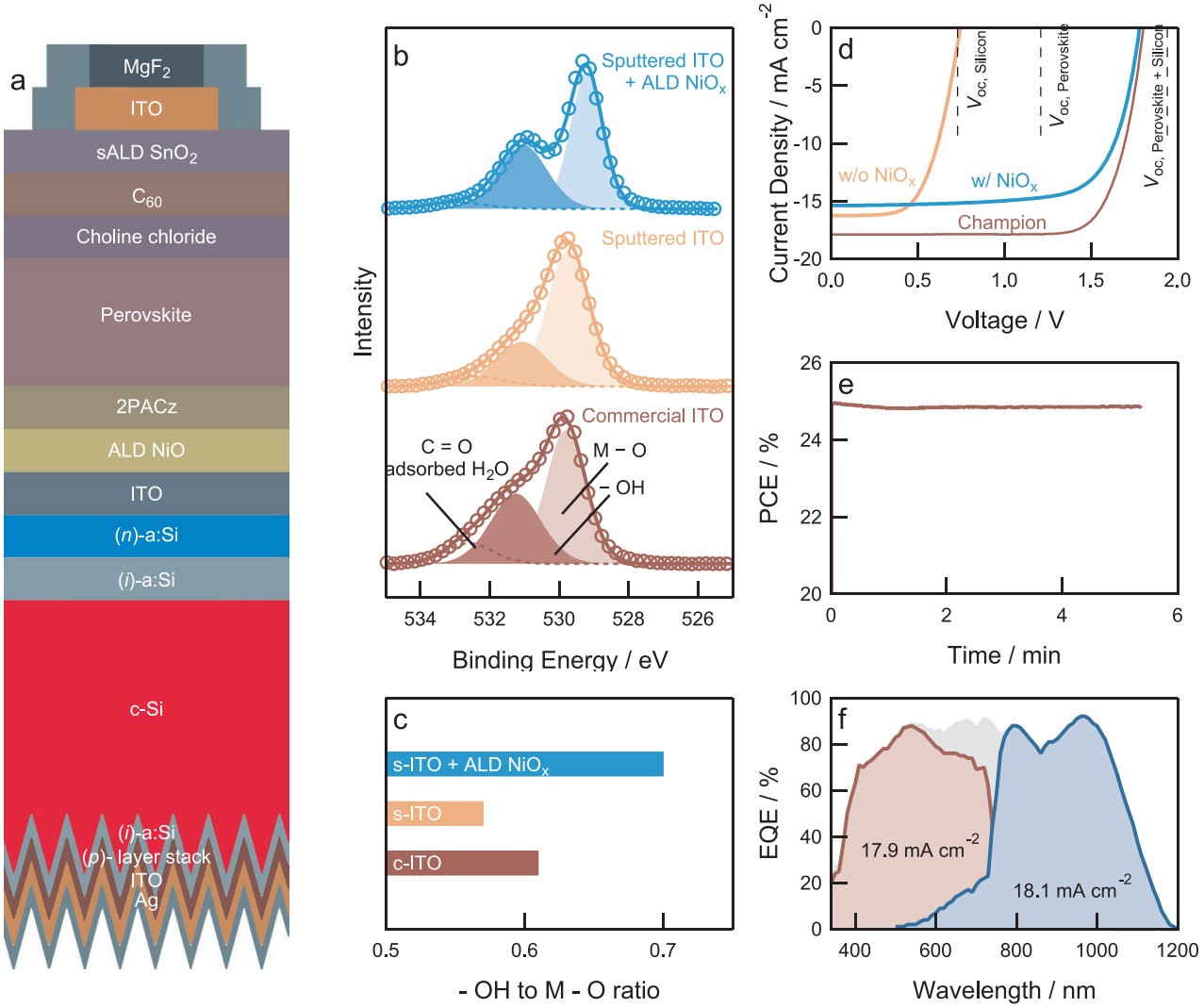

Figure 3. Monolithic perovskite-silicon tandem solar cell. a) Schematic of monolithic tandem device. b) X-ray photoelectron spectra (O1s) of commercial ITO, sputtered ITO, and sputtered ITO with an 8 nm-thick ALD-NiO interlayer. Spectral fits for metal oxide M–O and hydroxyl groups (–OH) are identified. c) –OH to M–O ratios derived from panel (b). d) Current-density versus voltage curves of tandem solar cells without (w/o) or with (w/) ALD-NiO interlayer, and champion device. e) Maximum power point tracking data of perovskite-silicon tandem solar cell. f) External quantum efficiency (EQE) spectrum of perovskite-silicon tandem solar cell. For each sub-cell the integrated short-circuit current density (J_{sc}) is indicated.

cell. The system was operated over 18 h of continuous illumination (Figure 4b), and subsequently simulating three 12 h diurnal cycles (Figure 4c). The system shows a stable output (STH) at the same potential as above (1.41 V) during 18 h of continuous illumination. The average output current of the solar cell was 18.0 mA, corresponding to a solar to hydrogen efficiency of 21.5% as calculated from:

$$\mathrm{STH} = \frac{1.23 I_{\mathrm{op}} \eta_{\mathrm{far}}}{A_{\mathrm{sc}} P_{\mathrm{in}}} \quad (1)$$

where I_{op} is the average operating current (18.0 mA), η_{far} = 0.999, A_{sc} the solar cell area (1 cm^2), and P_{in} the irradiance (103 mW cm^{-2}).[23] The Tafel slope of the electrochemical system is 37.3 mV dec^{-1} and the contact resistance is 369 mΩ cm^2. This would amount to about 27 mV increased potential if the area of the electrochemical and photovoltaic components were equal and increase the operating potential from 1.411 to 1.438 V, and reduce the current from 17.5 to 17.3 mA cm^{-2} (at 1-Sun intensity). This would lower the efficiency marginally from 21.5% to 21.3%.

The stability of the solar-assisted water splitting system was explored in multiple diurnal (12 h on–off) cycling.[24] Figure 4c further shows stable current and potential during the 72 h measurement window with similar irradiation conditions, indicating that the system is able to operate through several day-night cycles without loss of performance. The EC and PV units were characterized after the cumulative 90 h of operation; the polarization curve (EC) and current density versus voltage curves (PV) are nearly identical to initial measurements (Figure S3, Supporting Information), indicating that both systems retain their original performance, and that the operating potential of the integrated system remains unchanged. The shown stability

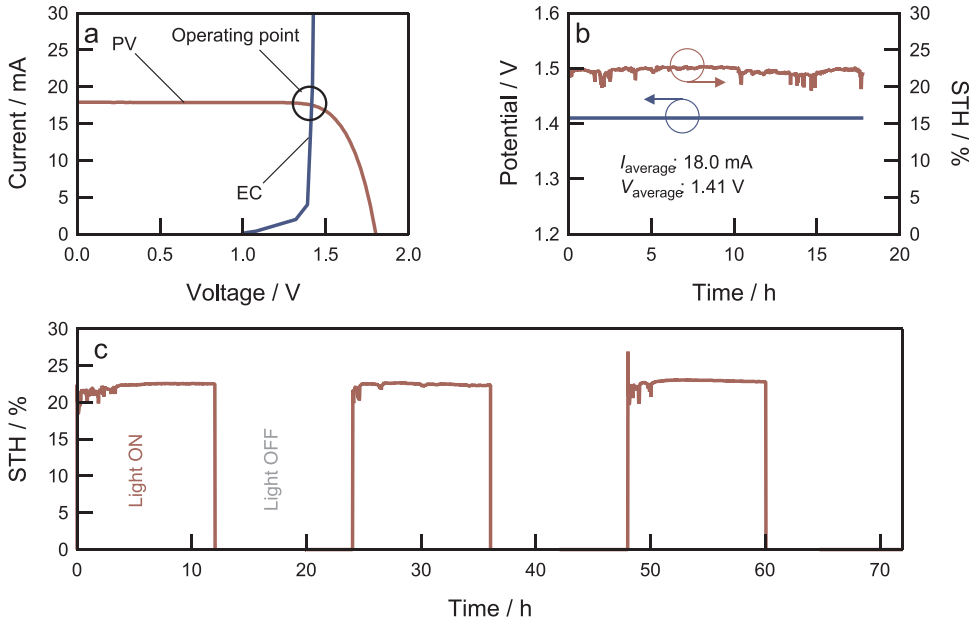

Figure 4. Continuous solar-assisted water splitting. a) Overlap of the *J–V* curve of the perovskite-silicon tandem solar cell with the polarization curve of the electrochemical flow cell. b) Solar-to-hydrogen conversion as a function of time using integrated PV-EC system over 18 h continuous operation at approx. 1-Sun equivalent light intensity. c) Diurnal cycling of PV-EC system (12 h light and 12 h dark) for a total of 72 h at approx. 1-Sun equivalent light intensity. Fluctuations in STH traces in panels (b) and (c) arise from fluctuations in lamp intensity during the operation of the device.

is greater than most reports in the literature with only a few reports showing system stabilities over 90 h.[5,8,11–13,21,22,25–34] Nonetheless, degradation of the individual components cannot be overlooked if the duration of the measurements is extended.

3. Conclusions

This work describes an integrated solar-assisted water splitting system using a flow electrochemical cell and a monolithic perovskite-silicon tandem solar cell, delivering an STH efficiency >21%. This STH efficiency is the highest reported for systems operating at approx. 1-Sun equivalent light intensity, and among the highest reported across a variety of combinations of EC and PV systems (Figure 1 and Table S1, Supporting Information). Specifically, to the best of our knowledge, this work is the first to demonstrate an efficient flow electrochemical cell operated without any light concentration techniques. Light concentration techniques are typically employed for systems using flow electrochemical cells, however, in this work, this was not required as the monolithic perovskite-silicon tandem solar cell generates a high current (≈18 mA) that allows the operation of the flow electrochemical cell at an operating potential over 1.4 V, which is close to the maximum power point of the solar cell. Despite the use of less abundant electrocatalysts, the high STH efficiency, the absence of light-concentration methods, and the use of low-cost monolithic perovskite–silicon tandem photovoltaics demonstrate a potential route to produce low-cost H_2.[35] Moreover, optimizing the EC/PV area ratio can be beneficial in terms of material cost in practical applications while maintaining high STH. In this work, a reduction of the EC/PV area ratio from 4 to 1 would imply only a minor drop in STH (21.5% to 21.3%). Recent efforts to develop earth-abundant electrocatalytic materials for use in electrochemical cells can further be used to construct low-cost electrochemical systems, augmenting the economic viability of solar-assisted H_2 production.[36]

Supporting Information

Supporting Information is available from the Wiley Online Library or from the author.

Acknowledgements

K.D., B.B., and Y.Z. contributed equally to this work. The authors thank Ludovico Riccardi for help with device schematics and Pauline Schmit for preparing the MEA for cross-section SEM. The authors acknowledge the Netherlands Organization for Scientific Research (NWO) for funding through the Joint Solar Programme III (Project 680.91.011) and the NWO Spinoza grant. The research further received funding from the European Union's Horizon 2020 Research and Innovation Programme under the Marie Skłodowska–Curie grant agreement No 765376 (eSCALED). N.P. and M.C. acknowledge the financial support from "PERCspective", specifically for the optimization of the NiO ALD process; the project is part of the Top consortia for Knowledge and Innovation (TKI) Solar Energy program (TEUE119005) of the Ministry of Economic Affairs of The Netherlands. M.C. acknowledged support from the NWO Aspasia program.

Conflict of Interest

The authors declare no conflict of interest.

Data Availability Statement

The data that support the findings of this study are available from the corresponding author upon reasonable request.

Keywords

electrochemical cell, electrochemical water splitting, hydrogen evolution, perovskite-silicon tandem solar cell

Received: July 11, 2022
Revised: August 21, 2022
Published online:

[1] International Energy Agency, World Energy Outlook 2020, Paris, **2020**.
[2] F. Lehner, D. Hart, in *Electrochemical Power Sources Fundamentals Systems Application*, Elsevier, New York **2022**, pp. 1–36.
[3] International Energy Agency, *The Future of Hydrogen*, Paris, **2019**, https://www.iea.org/reports/the-future-of-hydrogen (accessed: July 2022).
[4] C. A. Rodriguez, M. A. Modestino, D. Psaltis, C. Moser, *Energy Environ. Sci.* **2014**, *7*, 3828.
[5] Y. Shi, T. Y. Hsieh, M. A. Hoque, W. Cambarau, S. Narbey, C. Gimbert-Surinãch, E. Palomares, M. Lanza, A. Llobet, *ACS Appl. Mater. Interfaces* **2020**, *12*, 55856.
[6] A. Godula-Jopek, *Hydrogen Production: By Electrolysis*, Wiley-VCH, Weinheim, Germany **2015**.
[7] M. T. M. Koper, *J. Electroanal. Chem.* **2011**, *660*, 254.
[8] J. Jia, L. C. Seitz, J. D. Benck, Y. Huo, Y. Chen, J. W. D. Ng, T. Bilir, J. S. Harris, T. F. Jaramillo, *Nat. Commun.* **2016**, *7*, 13237.
[9] M. T. Hörantner, T. Leijtens, M. E. Ziffer, G. E. Eperon, M. G. Christoforo, M. D. McGehee, H. J. Snaith, *ACS Energy Lett.*. **2017**, *2*, 2506.
[10] A. Al-Ashouri, E. Köhnen, B. Li, A. Magomedov, H. Hempel, P. Caprioglio, J. A. Márquez, A. B. M. Vilches, E. Kasparavicius, J. A. Smith, N. Phung, D. Menzel, M. Grischek, L. Kegelmann, D. Skroblin, C. Gollwitzer, T. Malinauskas, M. Jošt, G. Matič, B. Rech, R. Schlatmann, M. Topič, L. Korte, A. Abate, B. Stannowski, D. Neher, M. Stolterfoht, T. Unold, V. Getautis, S. Albrecht, *Science* **2020**, *370*, 1300.
[11] J. Gao, F. Sahli, C. Liu, D. Ren, X. Guo, J. Werner, Q. Jeangros, S. M. Zakeeruddin, C. Ballif, M. Grätzel, J. Luo, *Joule* **2019**, *3*, 2930.
[12] Z. Li, S. Wu, J. Zhang, K. C. Lee, H. Lei, F. Lin, Z. Wang, Z. Zhu, A. K. Y. Jen, *Adv. Energy Mater.* **2020**, *10*, 2000361.
[13] Y. Wang, A. Sharma, T. Duong, H. Arandiyan, T. Zhao, D. Zhang, Z. Su, M. Garbrecht, F. J. Beck, S. Karuturi, C. Zhao, K. Catchpole, *Adv. Energy Mater.* **2021**, *11*, 2101053.
[14] S. Song, H. Zhang, X. Ma, Z. Shao, R. T. Baker, B. Yi, *Int. J. Hydrogen Energy* **2008**, *33*, 4955.
[15] S. Cherevko, S. Geiger, O. Kasian, N. Kulyk, J. P. Grote, A. Savan, B. R. Shrestha, S. Merzlikin, B. Breitbach, A. Ludwig, K. J. J. Mayrhofer, *Catal. Today* **2016**, *262*, 170.
[16] X. Zheng, B. Chen, J. Dai, Y. Fang, Y. Bai, Y. Lin, H. Wei, X. C. Zeng, J. Huang, *Nat. Energy* **2017**, *2*, 17102.
[17] K. Datta, J. Wang, D. Zhang, V. Zardetto, W. H. M. Remmerswaal, C. H. L. Weijtens, M. M. Wienk, R. A. J. Janssen, *Adv. Mater.* **2022**, *34*, 2110053.
[18] Y. Liu, Y. Li, Y. Wu, G. Yang, L. Mazzarella, P. Procel-Moya, A. C. Tamboli, K. Weber, M. Boccard, O. Isabella, X. Yang, B. Sun, *Mater. Sci. Eng., R* **2020**, *142*, 100579.
[19] A. Al-Ashouri, A. Magomedov, M. Roß, M. Jošt, M. Talaikis, G. Chistiakova, T. Bertram, J. A. Márquez, E. Köhnen, E. Kasparavičius, S. Levcenco, L. Gil-Escrig, C. J. Hages, R. Schlatmann, B. Rech, T. Malinauskas, T. Unold, C. A. Kaufmann, L. Korte, G. Niaura, V. Getautis, S. Albrecht, *Energy Environ. Sci.* **2019**, *12*, 3356.
[20] N. Phung, M. Verheijen, A. Todinova, K. Datta, M. Verhage, A. Al-Ashouri, H. Köbler, X. Li, A. Abate, S. Albrecht, M. Creatore, *ACS Appl. Mater. Interfaces* **2022**, *14*, 2166.
[21] H. Chen, L. Song, S. Ouyang, J. Wang, J. Lv, J. Ye, *Adv. Sci.* **2019**, *6*, 1900465.
[22] M. Lee, B. Turan, J. P. Becker, K. Welter, B. Klingebiel, E. Neumann, Y. J. Sohn, T. Merdzhanova, T. Kirchartz, F. Finger, U. Rau, S. Haas, *Adv. Sustainable Syst.* **2020**, *4*, 2000070.
[23] M. G. Walter, E. L. Warren, J. R. McKone, S. W. Boettcher, Q. Mi, E. A. Santori, N. S. Lewis, *Chem. Rev.* **2010**, *110*, 6446.
[24] S. A. Bonke, M. Wiechen, D. R. MacFarlane, L. Spiccia, *Energy Environ. Sci.* **2015**, *8*, 2791.
[25] S. Esiner, R. E. M. Willems, A. Furlan, W. Li, M. M. Wienk, R. A. J. Janssen, *J. Mater. Chem. A* **2015**, *3*, 23936.
[26] E. Verlage, S. Hu, R. Liu, R. J. R. Jones, K. Sun, C. Xiang, N. S. Lewis, H. A. Atwater, *Energy Environ. Sci.* **2015**, *8*, 3166.
[27] S. Rau, S. Vierrath, J. Ohlmann, A. Fallisch, D. Lackner, F. Dimroth, T. Smolinka, *Energy Technol.* **2014**, *2*, 43.
[28] C. R. Cox, J. Z. Lee, D. G. Nocera, T. Buonassisi, *Proc. Natl. Acad. Sci. USA* **2014**, *111*, 14057.
[29] J.-W. Schüttauf, M. A. Modestino, E. Chinello, D. Lambelet, A. Delfino, D. Dominé, A. Faes, M. Despeisse, J. Bailat, D. Psaltis, C. Moser, C. Ballif, *J. Electrochem. Soc.* **2016**, *163*, F1177.
[30] S. H. Hsu, J. Miao, L. Zhang, J. Gao, H. Wang, H. Tao, S. F. Hung, A. Vasileff, S. Z. Qiao, B. Liu, *Adv. Mater.* **2018**, *30*, 1707261.
[31] S. K. Karuturi, H. Shen, A. Sharma, F. J. Beck, P. Varadhan, T. Duong, P. R. Narangari, D. Zhang, Y. Wan, J. H. He, H. H. Tan, C. Jagadish, K. Catchpole, *Adv. Energy Mater.* **2020**, *10*, 2000772.
[32] H. Park, I. J. Park, M. G. Lee, K. C. Kwon, S. P. Hong, D. H. Kim, S. A. Lee, T. H. Lee, C. Kim, C. W. Moon, D. Y. Son, G. H. Jung, H. S. Yang, J. J. R. Lee, J. J. R. Lee, N. G. Park, S. Y. Kim, J. Y. Kim, H. W. Jang, *ACS Appl. Mater. Interfaces* **2019**, *11*, 33835.
[33] Y. Kuang, M. J. Kenney, Y. Meng, W. H. Hung, Y. Liu, J. E. Huang, R. Prasanna, P. Li, Y. Li, L. Wang, M. C. Lin, M. D. McGehee, X. Sun, H. Dai, *Proc. Natl. Acad. Sci. USA* **2019**, *116*, 6624.
[34] J. L. Young, M. A. Steiner, H. Döscher, R. M. France, J. A. Turner, T. G. Deutsch, *Nat. Energy* **2017**, *2*, 17028.
[35] C. Messmer, B. S. Goraya, S. Nold, P. S. C. Schulze, V. Sittinger, J. Schön, J. C. Goldschmidt, M. Bivour, S. W. Glunz, M. Hermle, *Prog. Photovoltaics* **2021**, *29*, 744.
[36] I. Roger, M. A. Shipman, M. D. Symes, *Nat. Rev. Chem.* **2017**, *1*, 0003.